EXTENSIONS AND IMPROVEMENTS OF XTRAN3S

C. J. Borland
Boeing Military Airplane Co.
Seattle, Washington

SUMMARY

This paper will summarize recent work that has been performed under a NASA Langley Contract NAS1-17864, "Additional Development of the XTRAN3S Computer Program." Work on this code, for steady and unsteady aerodynamic and aeroelastic analysis in the transonic flow regime, has concentrated in four areas:

1) Maintenance of the XTRAN3S code, including correction of errors, enhancement of operational capability, and installation on the Cray X-MP system at Wright-Patterson Air Force Base;
2) Extension of the vectorization concepts in XTRAN3S to include additional areas of the code for improved execution speed;
3) Modification of the XTRAN3S algorithm for improved numerical stability for swept, tapered wing cases and improved computational efficiency;
4) Extension of the wing-only version of XTRAN3S to include pylon and nacelle or external store capability.

- MISCELLANEOUS PROGRAM CORRECTIONS & ENHANCEMENTS
- IMPROVED VECTORIZATION OF XTRAN3S
- ALGORITHM IMPROVEMENT
- DEVELOPMENT OF WING/PYLON/STORE CAPABILITY

MISCELLANEOUS PROGRAM CORRECTIONS

This figure lists the various UPDATE correction sets for correction of errors in the XTRAN3S code. These correction sets are to be applied to BCS Version 1.6 (equivalent to Langley Version 1.5) of the XTRAN3S code.

UPDATE NAME	FUNCTION
EXTLOFT	CORRECTS LOFTING PROCEDURE FOR EXTRAPOLATION OF AIRFOIL DATA
VISCORR	CORRECTS ERROR IN WEDGE PARAMETER DEFINITION
FIXPROMAT	CORRECTS DATA INPUT ERROR FOR INERTIA MATRIX
MISCFIX	CORRECTS GEOMETRY DEFINITION ERROR, MODIFIES CPRESS AND CFOMO TO ACCOUNT FOR MODIFIED GRID, AND VARIABLE DIMENSION ERROR IN ZSWEEP
ENCODE	CORRECTS LABELING ERROR IN TIME HISTORY OUTPUT
VECTCORR	CORRECTS INITIALIZATION ERROR IN VECTORIZATION
PARMGEO	PROVIDES VARIABLE DIMENSION FOR NUMBER OF POINTS ON AIRFOIL

MISCELLANEOUS PROGRAM ENHANCEMENTS

This and the following figure list the UPDATE correction sets for improvement of XTRAN3S operational features. This group of correction sets, plus the previous list of error correction modifications, constitute upgrade of the XTRAN3S code from Version 1.6 to Version 1.10.

UPDATE NAME	FUNCTION
BCS17	ALLOWS ALTERNATE INPUT FILE FOR AEROELASTIC DATA AND ADDS SELECTIVE DEGREE-OF-FREEDOM MATRIX
CONTROL	ADDS 2 SOLUTION TASKS: (A) STATIC RIGID ANALYSIS WITH CONTROL SURFACE DEFLECTION (B) STATIC AEROELASTIC ANALYSIS WITH CONTROL SURFACE DEFLECTION
INVERR	ADDS OUTPUT OF AEROELASTIC DATA
TASKCORR	UPDATES DOCUMENTATION AND LOGIC FOR CONTROL UPDATE
INTEQM	ADD OPTION FOR INTEGRATION OF EQUATIONS OF MOTION FOR ZERO AIR FORCES

MISCELLANEOUS PROGRAM ENHANCEMENTS (continued)

UPDATE NAME	FUNCTION
NEWBL	REMOVES EFFECT OF SHOCK SWEEP ON BOUNDARY LATER CALCULATION
SHOCKFIX	PROVIDES PROPER SHOCK PLACEMENT FOR NEWBL
VERS110	UPDATES PROGRAM BANNERS TO VERSION 1.10
WRTWRNS	ADDS ADDITIONAL ERROR DIAGNOSTICS
WPAFB1	UPDATES FOR INSTALLATION AT WPAFB.
WPAFB2	

IMPROVED VECTORIZATION OF XTRAN3S

The original version of XTRAN3S was developed using the CDC 7600 computer. During the code development period, advanced vector machines, such as the VPS-32 and CRAY-1S and later the CRAY X-MP became available. The code was adapted to operate on these machines, but only minimal changes to the code were performed to take advantage of "implicit" vectorization, i.e., those portions of the code that could easily be adapted to vector computation through the existing nature of the computational algorithm.

Later studies with a pilot code version of XTRAN3S, operational on the CRAY-1S, showed that at least a factor of two improvements in computational efficiency could be achieved by rearrangement of operations to permit a larger degree of implicit (or automatic) vectorization. (This represents a speed-up factor of almost five compared to an unvectorized or scalar code operating on the same machine.) These concepts are generally applicable, but not directly transportable, to the VPS-32 version of the code, since VPS-32 requires longer vectors than the CRAY-1S to achieve improved efficiency when compared with scalar computations. The improved vectorization scheme has now been implemented on the CRAY X-MP in Version 1.10 of XTRAN3S.

In this section of the presentation the original algorithm will be described with respect to its implications for vectorization. Then the modifications necessary to achieve a higher degree of vectorization on the CRAY X-MP will be discussed.

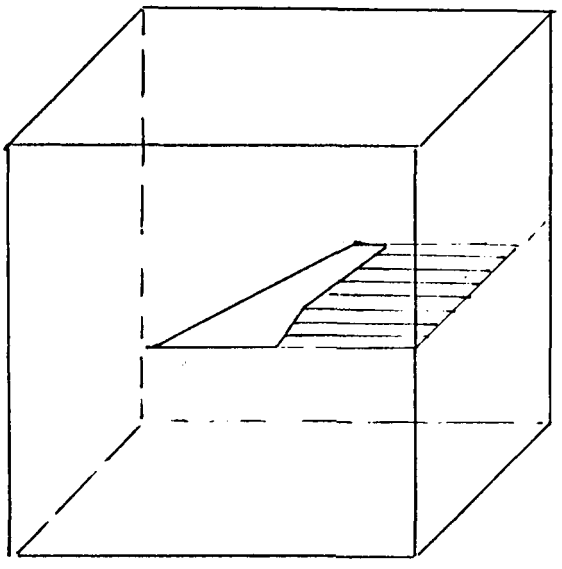

PHYSICAL SPACE

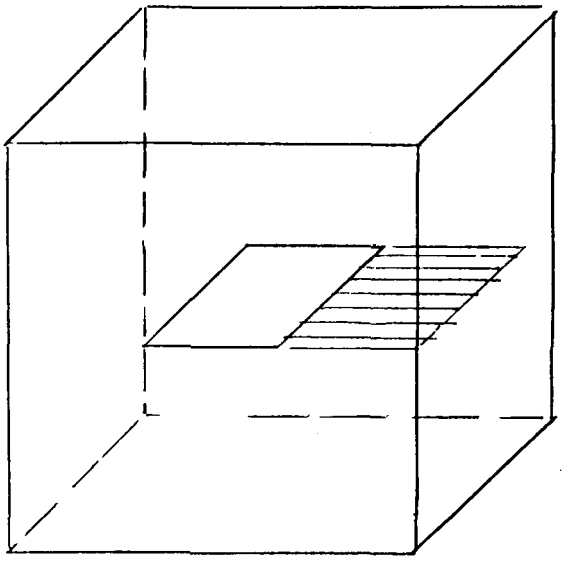

COMPUTATIONAL SPACE

ORIGINAL ALGORITHM STORAGE SCHEME (Version 1.5)

In the original version of XTRAN3S, the equations for the X-sweep are solved sequentially for each Y mesh point, with a constant Z mesh point location. Thus for the default values of $N_X = 60$, $N_Y = 20$, $N_Z = 40$, 20 equations of length 60 are solved for each X-Y plane. Then, for the same X-Y plane, the Y-sweep equations (60 equations of length 20) are solved sequentially in the downstream (increasing X) direction due to the presence of the backward spatial or "upwind" difference approximation to ϕ_{xt}. This process is then repeated for the next X-Y plane in the increasing Z direction. The Z-sweep is performed by accessing the data, formulating the equations, and solving for each X-Z plane sequentially in the increasing downstream direction, with the process then repeated for the next plane in the increasing η direction. Since solutions of the Z-sweep equations, ϕ^{n+1}, are dependent on ϕ^n, ϕ^{n-1} and the solution of the Y-sweep equations $\tilde{\phi}$, but not on the solutions to the X-sweep equations, $\tilde{\phi}$ need not be stored in a three-dimensional array.

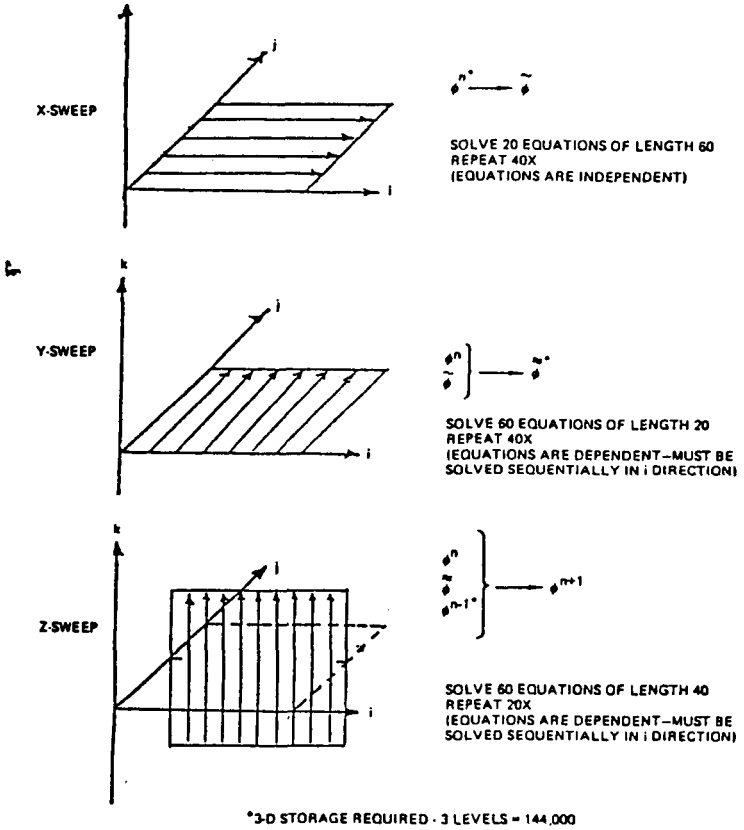

*3-D STORAGE REQUIRED - 3 LEVELS = 144,000

MODIFIED ALGORITHM STORAGE SCHEME (Version 1.10)

For the CRAY X-MP, the scheme illustrated in this figure has been adopted. For the X-sweep, data is accessed for each Y-Z plane (rather than each X-Y plane), and vectorized solution is performed in the Z direction, i.e., each step in the solution is a vector operation of length 40. This is then repeated for the next Y-Z plane, and the intermediate result $\tilde{\phi}$ is stored in a three-dimensional array. For the Y sweeps, the data is accessed in the Y-Z planes, and a vectorized solution of length 40 is again performed in the Z direction, with the results $\tilde{\phi}$ stored in a three-dimensional array. Finally, the Z-sweeps are performed as a vectorized solution of length 20 in the Y direction, and the advanced values of the potential ϕ^{n+1} are stored in place of the values ϕ^n at the previous time step. It should be noted that four three-dimensional "levels" of storage, ϕ^n, ϕ^{n-1}, $\tilde{\phi}$ and $\tilde{\phi}$ are required for this scheme, compared with three for the original scheme. In addition, however, nine additional three-dimensional arrays for vector equation coefficients and right-hand sides have been stored to improve efficiency and decrease the amount of re-calculation required. For the default mesh, the amount of storage for three-dimensional arrays has increased from 144,000 to 624,000. The total storage requirement has thus increased from about one-half million words to over one million words. Because of the larger amounts of storage available on both the CRAY X-MP and VPS-32, compared to the CDC 7600, this has caused no difficulty.

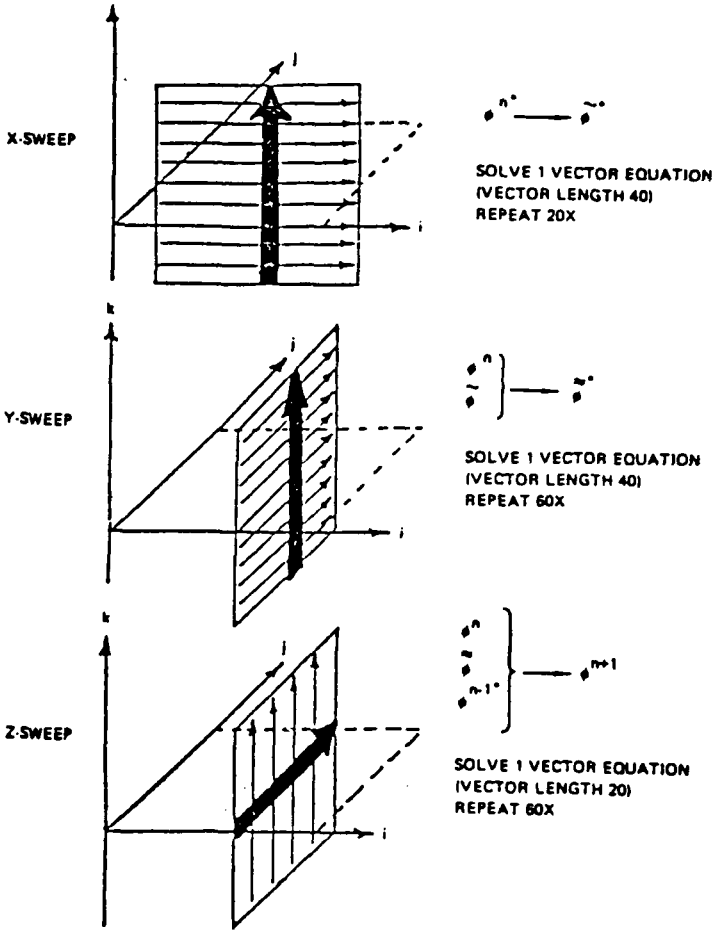

*3-D STORAGE REQUIRED - 4 LEVELS + 9 COEFFICIENTS = 624,000

ORIGINAL PAGE IS
OF POOR QUALITY

VECTORIZATION OF NASA WING-BODY MODIFICATION

This figure shows the improvements that can be achieved by careful attention to the use of vectorization concepts. The NASA-Langley developed wing-body modification update was installed in both the standard Version 1.5 and improved Version 1.10. Due to the use of conditional branching within computation loops (DO-loops), vectorization was inhibited. Version 1.5 took more than twice as long to run a wing-body case as a wing-alone case with the same dimensions, and Version 1.10 took more than three times as long. (The unmodified Version 1.10 runs more than twice as fast as Version 1.5). When the conditional branches were constrained to the outside of computation loops, permitting vectorization to occur, considerable speed-up was achieved. A wing-body case can now be run using Version 1.10 with only an increase of 4% over the cost of a wing-alone case. These constraints are applied in all the modification of XTRAN3S described below.

VERSION/CASE	WING ONLY	WING-BODY
1.5	1.0	-
1.5 + W-B	1.05	2.18
1.10	.43	-
1.10 + W-B	1.69	1.744
1.10 + W-B (VECTORIZED)	.43	.45

(NORMALIZED CP SEC/ITERATION)

XTRAN3S ALGORITHM IMPROVEMENT

The XTRAN3S code solves the modified transonic small disturbance equation shown in this figure. After transforming the wing planform in Cartesian Coordinates (X, Y, Z) to a rectangular region in computation coordinates (ξ, η, ζ), the equation appears as shown below.

The underlined terms originate with the spanwise (Y-dependent) or cross (X-Y dependent) terms of the original equation, $G\phi_{y2}$ and $\phi y + H\phi_{x\phi y}$. The non-underlined terms depend only on original streamwise or normal derivatives. In the XTRAN3S algorithm, the original spanwise term $G\phi_{y2}$ was split into streamwise and transformed normal components. These terms were then treated separately with the streamwise component treated implicitly, and the normal component treated explicitly.

MODIFIED TRANSONIC SMALL DISTURBANCE EQ.

$$\frac{\partial}{\partial t}\left(-A\varphi_t - B\varphi_x\right) + \frac{\partial}{\partial x}\left(E\varphi_x + F\varphi_x^2 + \underline{G\varphi_y^2}\right)$$

$$+ \frac{\partial}{\partial y}\left(\underline{\varphi_y + H\varphi_x\varphi_y}\right) + \frac{\partial}{\partial z}\left(\varphi_z\right) = 0$$

TRANSFORMING TO $\xi = \xi(x,y)\ ;\ \eta = y\ ;\ \zeta = z\ ;\ \tau = t$

$$\frac{\partial}{\partial \tau}\left(-\frac{A}{\xi_x}\varphi_\tau - B\varphi_\xi\right)$$

$$+ \frac{\partial}{\partial \xi}\left\{E\xi_x\varphi_\xi + F\xi_x^2\varphi_\xi^2 + \underline{G\left(\xi_y\varphi_\xi + \varphi_\eta\right)^2 + \frac{\xi_y}{\xi_x}\left(\xi_y\varphi_\xi + \varphi_\eta\right) + H\xi_y\varphi_\xi\left(\xi_y\varphi_\xi + \varphi_\eta\right)}\right\}$$

$$+ \frac{\partial}{\partial \eta}\left\{\underline{\frac{1}{\xi_x}\left(\xi_y\varphi_\xi + \varphi_\eta\right) + H\varphi_\xi\left(\xi_y\varphi_\xi + \varphi_\eta\right)}\right\} + \frac{\partial}{\partial \zeta}\left\{\frac{1}{\xi_x}\varphi_\zeta\right\} = 0$$

The equation can be rewritten as shown by recollecting terms by coefficients of like-terms. Here a and b are the original (x-direction) streamwise terms of the governing equations, and $\hat{a}$, $\hat{b}$, etc., contain coefficients based on the spanwise terms of the equation. It has been previously noted that a time-accurate, fully conservative, implicit treatment can only be performed on the terms

$$\frac{\partial}{\partial \xi}\left(\hat{a}\phi_{\xi} + \hat{b}\phi_{\xi}^{2}\right) \quad \text{and} \quad \frac{\partial}{\partial \eta}\left(\frac{1}{\xi}\phi_{\eta}\right)$$

The remaining terms can be differenced in a fully conservative explicit fashion, or in a partially conservative implicit fashion. In the original XTRAN3S algorithm, only the cross-term $\frac{\partial}{\partial \xi}(G\phi_{\eta}^{2})$ is so treated; the remaining terms are treated explicitly. In the present study, several different combinations of implicit and explicit difference treatments have been investigated. By examining the coefficients it can be seen that certain terms which were treated explicitly in the original XTRAN3S algorithm can be treated implicitly without loss of accuracy (i.e., without losing the conservation form of the equation). It has also been noted by Batina that only the original streamwise terms, represented by the coefficients $\hat{a}$ and $\hat{b}$ should be included in the type-dependent difference scheme or in the definition of the shock point operator. This treatment of these terms corresponds directly to the original 2-dimensional method of Ballhaus and Goorjian known as LTRAN2.

RECOLLECTING TERMS:

$$\frac{\partial}{\partial \tau}\left(-\frac{A}{\xi_x}\varphi_t - B\varphi_\xi\right)$$

$$\frac{\partial}{\partial \xi}\left(\hat{a}\varphi_\xi + \hat{b}\varphi_\xi^2 + \hat{\hat{a}}\varphi_\xi + \hat{\hat{b}}\varphi_\xi^2 + \hat{c}\varphi_\eta + \hat{d}\varphi_\eta^2\right)$$

$$+ \frac{\partial}{\partial \eta}\left(\hat{e}\varphi_\xi + \hat{f}\varphi_\xi^2 + \hat{g}\varphi_\eta\right)$$

$$+ \frac{\partial}{\partial \zeta}\left(\hat{h}\varphi_\zeta\right) = 0$$

WHERE

$$\hat{a} = E\xi_x \qquad \hat{\hat{a}} = \xi_y^2/\xi_x + (2G+H)\xi_y\varphi_\eta \qquad \hat{b} = F\xi_x^2$$

$$\hat{\hat{b}} = (G+H)\xi_y^2 \,, \qquad \hat{c} = \xi_y/\xi_x \qquad \hat{d} = G$$

$$\hat{e} = \xi_y/\xi_x \qquad \hat{f} = H\xi_y \qquad \hat{g} = \frac{1}{\xi_x} + H\varphi_\xi \qquad \hat{h} = \frac{1}{\xi_x}$$

ORIGINAL ADI ALGORITHM

The transformed streamwise sweep for the original (Version 1.5) XTRAN3S algorithm is shown in this figure.

Here $D\xi$ is a type-dependent mixed difference operator based on the sign of $(\hat{a}^n + 2\,G\phi\xi^D)$, $\delta\xi$ is a central difference operator, $D\eta$ is a mixed difference operator based upon the sign of $2G_S(\delta_\eta \phi n)$.

ξ - SWEEP:

$$B\,\hat{\delta}_\xi\left(\frac{\tilde{\varphi}-\varphi^n}{\Delta t}\right) = D_\xi\left[a^n\left(\frac{\tilde{\varphi}_\xi-\varphi_\xi^n}{2}\right) + b\varphi_\xi^n\tilde{\varphi}_\xi\right]$$
$$+\ 2G_s\left(\delta_\eta\varphi^n\right)D_\eta\left(\hat{\delta}_\xi\varphi^n\right) + \delta_\eta\left(\frac{1}{\xi_x}\,\delta_\eta\varphi^n\right)$$
$$+\ \frac{1}{\xi_x}\,\delta_{\xi\xi}\varphi^n + \delta_\xi X^n + \delta_\eta Y^n$$

WHERE

$$X^n = G_N\left(\xi_y\varphi_\xi^n + \varphi_\eta\right)^2 + H\,\xi_y^2\varphi_\xi^{n2} + H\,\xi_y\varphi_\xi^n\varphi_\eta^n$$
$$+\ \xi_y/\xi_x\,\varphi_\eta^n + \xi_y^2/\xi_x\,\varphi_\xi^{n2}$$

$$Y^n = \xi_y/\xi_x\,\varphi_\xi^n + H\,\xi_y\varphi_\xi^{n2} + H\,\varphi_\xi^n\varphi_\eta^n$$

MODIFIED ADI ALGORITHM

The transformed streamwise sweep for the modified (Version 1.10) XTRAN3S algorithm is shown in this figure. Here it can be seen that all but one of the explicitly-treated streamwise derivative terms ($\delta_\xi X^n$) in the original algorithm can be treated implicitly. The remaining cross-derivative terms $\delta_\xi(\phi_\eta)$ or $\delta_\eta(\phi_\xi)$ must still be treated explicitly.

ξ - SWEEP:

$$B\,\overleftarrow{\delta}_\xi\left(\frac{\tilde{\varphi}-\varphi^n}{\Delta t}\right) = D_\xi\left[\hat{a}^n\left(\frac{\tilde{\varphi}_\xi+\varphi_\xi^n}{2}\right)+\hat{b}\,\varphi_\xi^n\,\tilde{\varphi}_\xi\right]$$

$$+\ \delta_\xi\left[\hat{\hat{a}}^n\left(\frac{\tilde{\varphi}_\xi+\varphi_\xi^n}{2}\right)+\hat{\hat{b}}\,\varphi_\xi^n\,\tilde{\varphi}_\xi\right]$$

$$+\ 2G\left(\delta_\eta\varphi^n\right)D_\eta\left(\overleftarrow{\delta}_\xi\varphi^n\right)+\delta_\eta\left(\frac{1}{\xi_x}\delta_\eta\varphi^n\right)$$

$$+\ \frac{1}{\xi_x}\delta_{\xi\xi}\varphi^n+\delta_\xi X^n+\delta_\eta Y^n$$

WHERE

$$X^n = \xi_y/\xi_x\,\varphi_\eta^n$$

$$Y^n = \xi_y/\xi_x\,\varphi_\xi^n + H\,\xi_y\,\varphi_\xi^2 + H\,\varphi_\xi^n\varphi_\eta^n$$

The transformed spanwise and vertical sweeps are unmodified in the new algorithm since these solutions are fully implicit.

η - SWEEP:

$$B\overleftarrow{\delta_\zeta}\left(\frac{\tilde{\tilde{\varphi}}-\varphi^n}{\Delta t}\right)=\frac{1}{2}\delta_\eta\left(\frac{1}{\xi_x}\delta_\eta\tilde{\tilde{\varphi}}-\frac{1}{\xi_x}\delta_\eta\varphi^n\right)$$

$$+\,G\left(\delta_\eta\varphi^n\right)D_\eta\left(\overleftarrow{\delta_\zeta}\tilde{\tilde{\varphi}}-\overleftarrow{\delta_\zeta}\varphi^n\right)$$

ζ - SWEEP:

$$\frac{A}{\xi_x}\left(\frac{\varphi^{n+1}-2\varphi^n+\varphi^{n-1}}{\Delta t^2}\right)+B\overleftarrow{\delta_\zeta}\left(\frac{\varphi^{n+1}-\tilde{\tilde{\varphi}}}{\Delta t}\right)$$

$$+\frac{1}{2}\cdot\frac{1}{\xi_x}\,\delta_{JJ}\left(\varphi^{n+1}-\varphi^n\right)$$

(THESE SWEEPS UNMODIFIED)

A-6E TEST PROBLEM

The modified ADI algorithm has been tested on the wing planform for the A-6E attack aircraft with a moderate sweep and taper. The computation time step could be increased by a factor of ten with numerical stability maintained. For a more severely swept and tapered planform (the F-5 wing) an increase of more than fifteen has been reported.

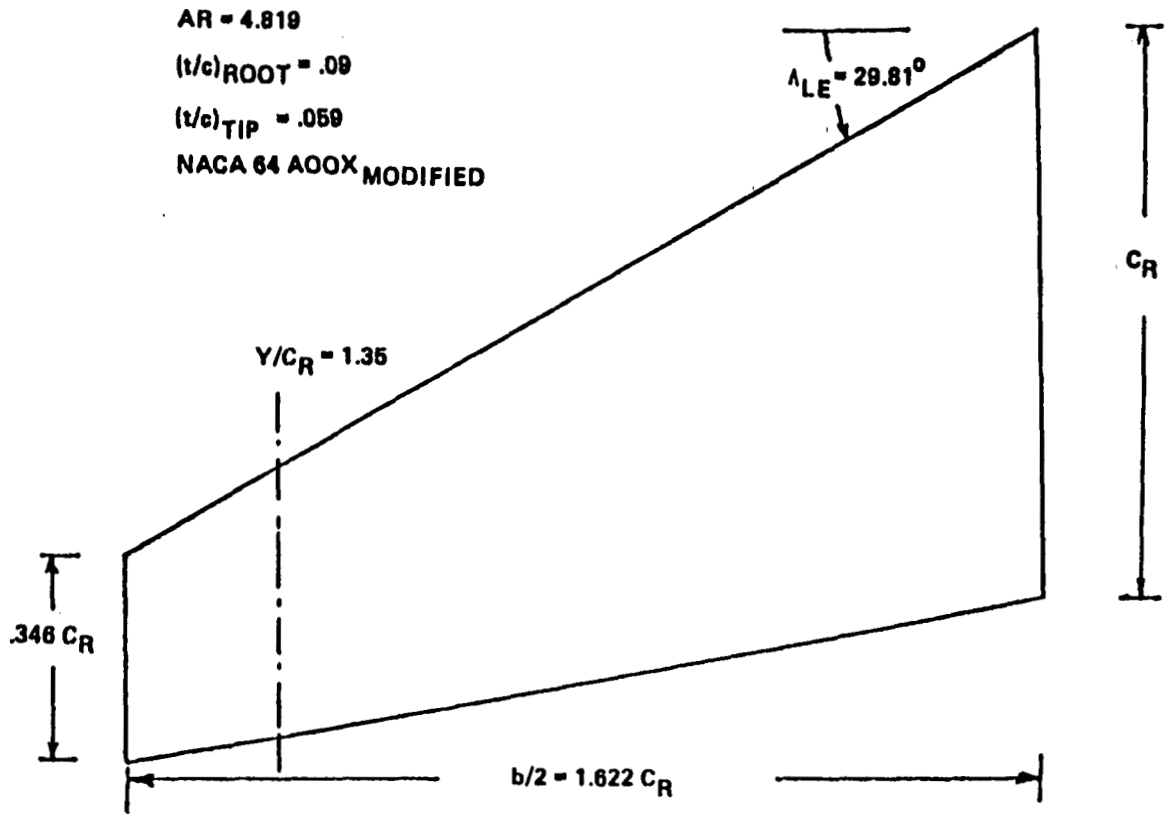

A-6E Planform in XTRAN3S Calculations

This figure shows the resulting steady pressure distributions for the original and modified ADI algorithms. In the modified algorithm the shock has moved one grid point upstream. Otherwise results are essentially identical.

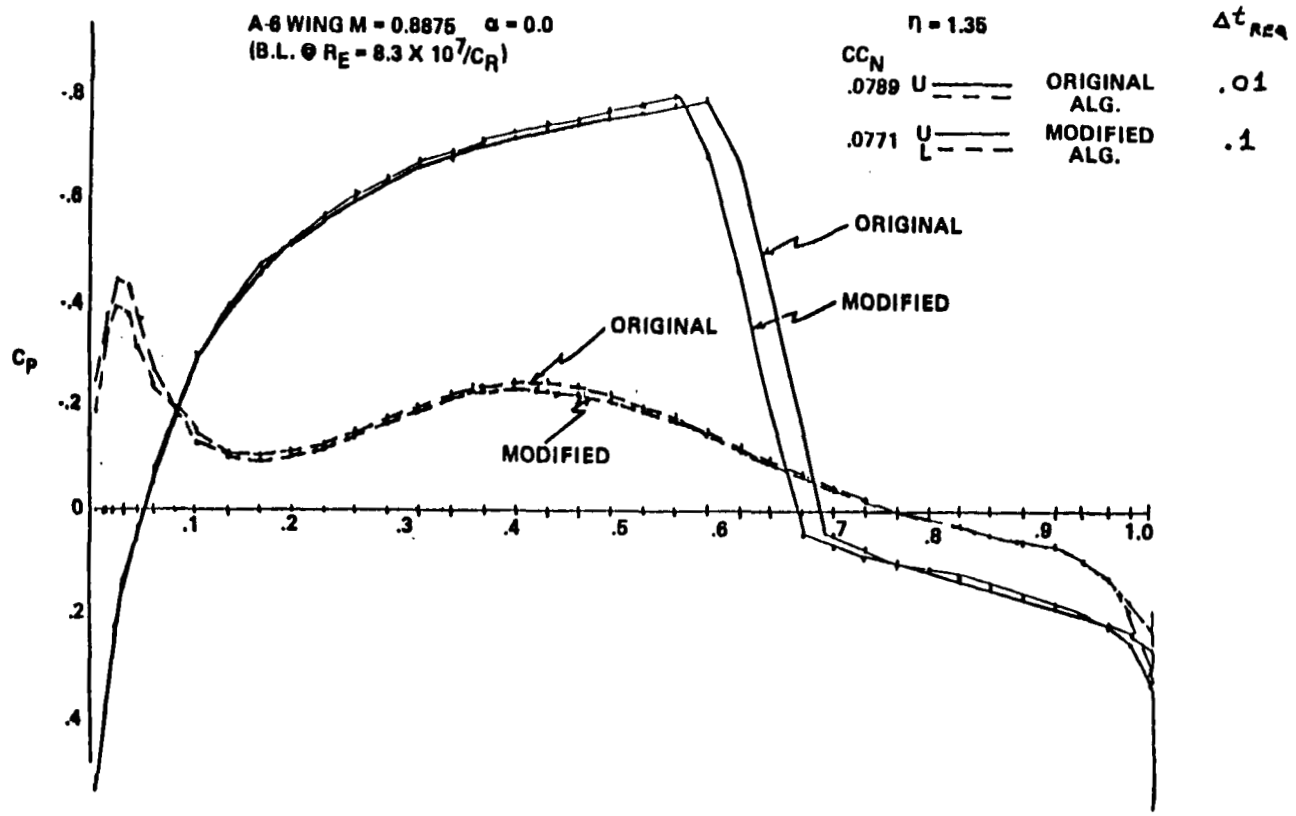

Comparison of Pressure Distribution Calculated by the Original and Revised XTRAN3S Algorithms

WING-PYLON STORE TRANSONIC ANALYSIS

This section of the presentation will describe the development and current status of a pylon/external store or nacelle capability in XTRAN3S.

Wing - Pylon - Store

Transonic Analysis

With XTRAN3S

A-6 WING WITH STORES

Flutter characteristics of military aircraft may be severely affected by the presence of external stores. These stores may affect the flow field characteristics as well as the structural dynamic characteristics of the aircraft. Flutter speeds with carriage of external stores are usually lower than for the clean wing and may require severe operational restrictions. This figure shows a schematic of the wing of the Navy A-6E attack aircraft. As a part of the flutter clearance program for the newly-designed graphite-epoxy A-6 Replacement Wing, Boeing performed wind tunnel tests on both rigid and aeroelastic transonic models. The A-6 wing is shown here with 2 -400 gallon external fuel tanks mounted on pylons under the wings at two inboard stations (the third station is used to mount a small air-air missile such as the AIM-9L Sidewinder). The wing is moderately swept and tapered. Simulations conducted to date with XTRAN3S did not include the inboard strake, fuselage, or nacelle.

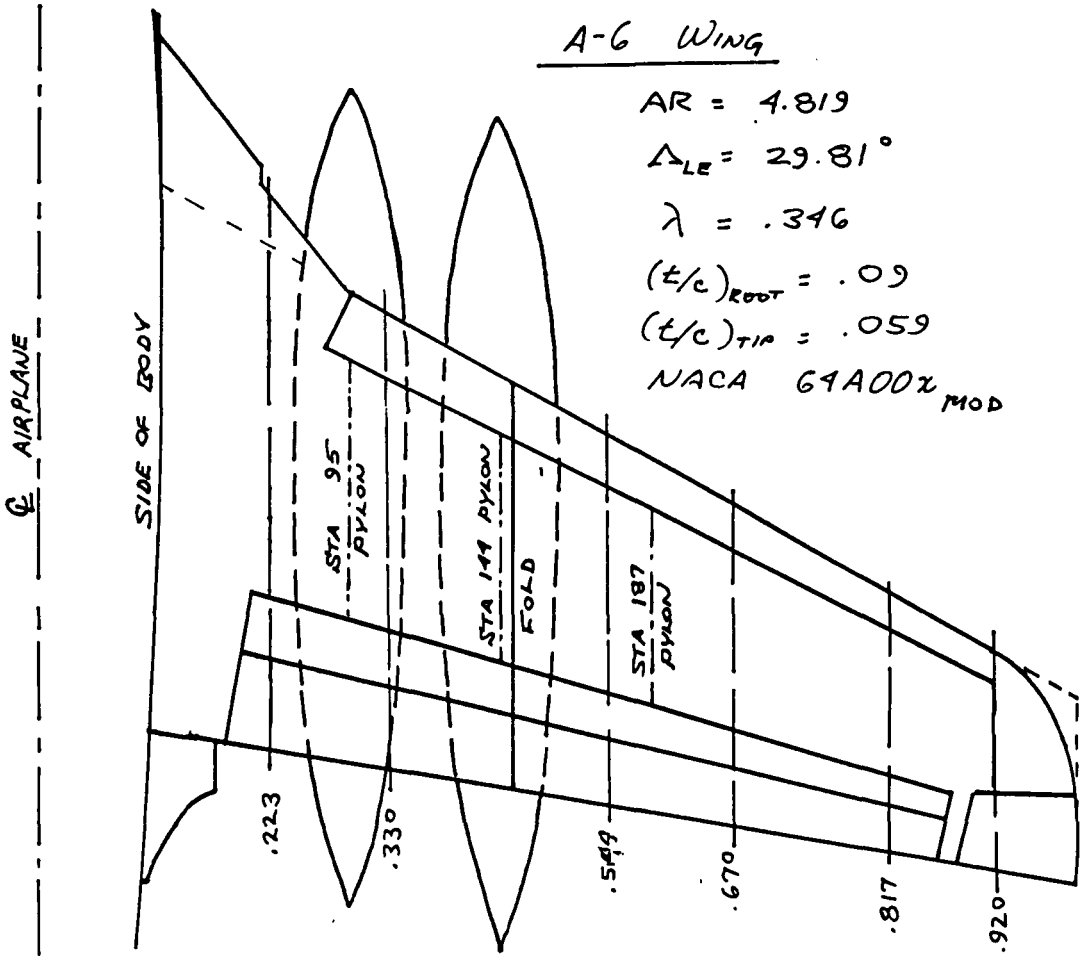

ORIGINAL PAGE IS
OF POOR QUALITY

As seen in this figure, aerodynamic interference due to the presence of the stores has a significant effect on the sectional lift distribution of the wing. (Symbols represent data from a static rigid test). Also shown is a prediction of the static lift curve slopes by XTRAN3S for the clean wing. Flutter results using the clean wing XTRAN3S aerodynamics and the clean wing test data as correction factors in an interfering modified strip theory analysis are essentially the same.

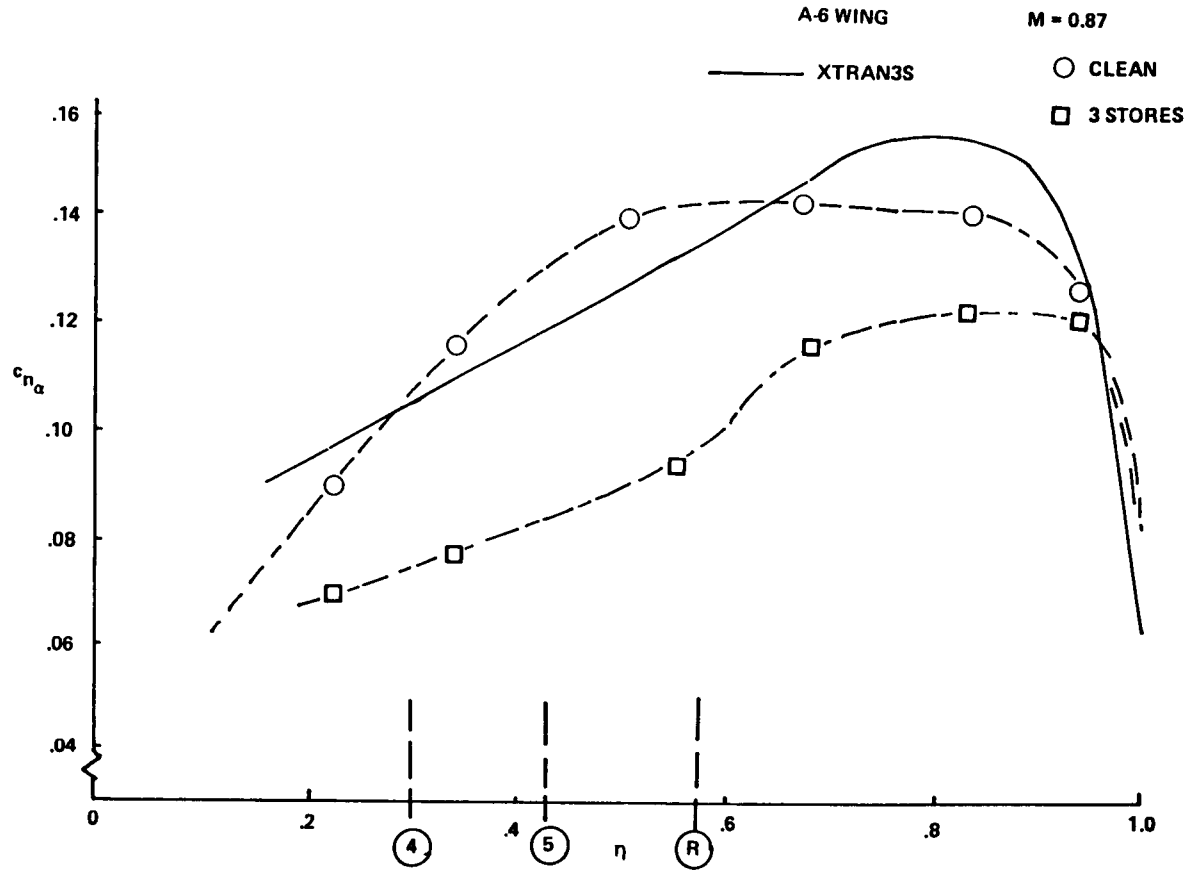

FLUTTER TEST COMPARISON - ONE STORE

In this figure, analysis of the A-6 wind tunnel flutter model tested in NASA's Transonic Dynamics Tunnel for both the "clean wing" and "stores on" aerodynamics correction factors (section lift curve slopes and aerodynamic centers) are compared with measured flutter dynamic pressures. The analysis for both sets of corrections shows the typical "transonic bucket" as a function of Mach number. The model test with an actual stores representing a single 300 gallon external fuel tank showed essentially no effect of Mach number - a completely unexpected result! An effort to explain this phenomenon, a "pencil store", or simulator with identical mass and inertia properties but minimum aerodynamic interference was also tested. Here the results showed the expected Mach effect of decreasing flutter speed up to a critical Mach number. A "no-flutter" run (not shown) at higher speeds demonstrated the classical transonic bucket behavior. Thus the importance of wing-store aerodynamic interference and potential aerodynamics of the store itself were demonstrated.

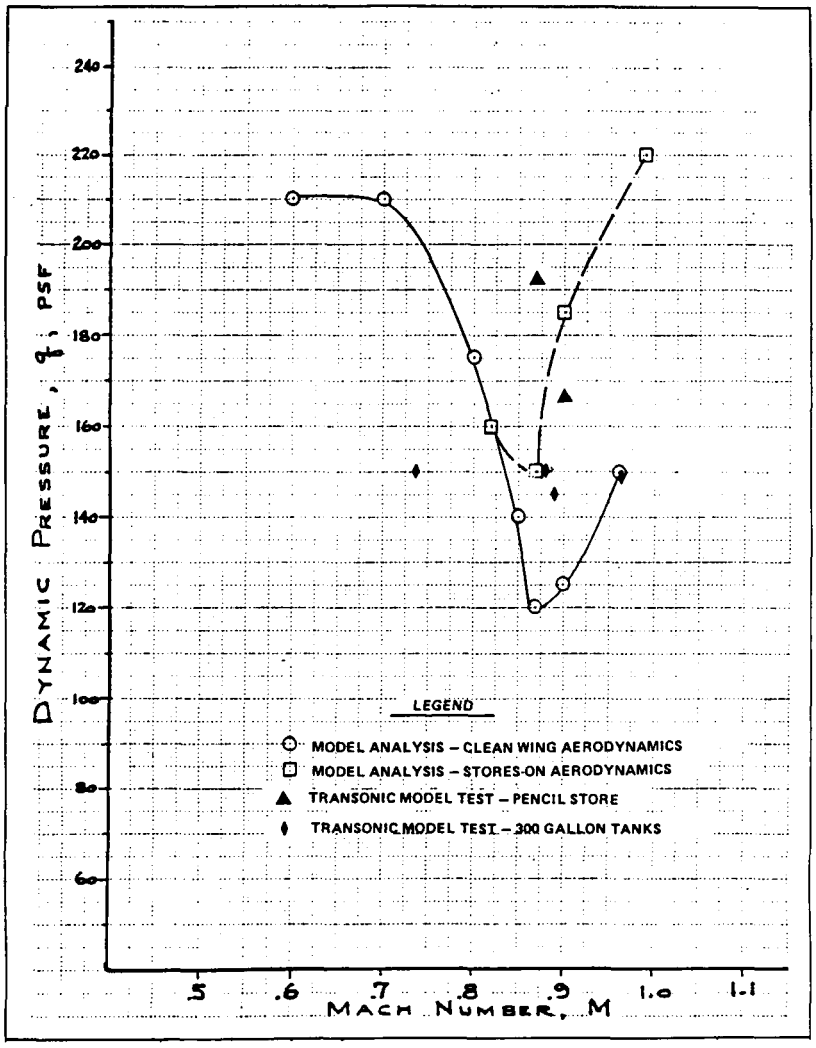

FLUTTER ANALYSIS,
300 GALLON TANK ON PYLON 5

FLUTTER TEST COMPARISON - TWO STORES

This figure shows a similar comparison of analysis and test results for two 300 gallon tanks and pencil stores. Although the measured flutter boundary shows a much higher Mach number for the same dynamic pressure at flutter (or vise versa), the bucket behavior for the pencil stores is again confirmed. The actual stores show no appreciable effect of Mach number on flutter. One principal difference between the actual stores and the simulators was the rapidity of the onset of flutter. With the actual stores, flutter was approached quite slowly with fairly long times to double amplitude (5-10 seconds) allowing good confirmation of actual flutter behavior without risk to the model. On the second flutter point shown with the simulators (at a q of 155 psf) violent flutter was encountered (.1 sec to double amplitude) and the model was destroyed.

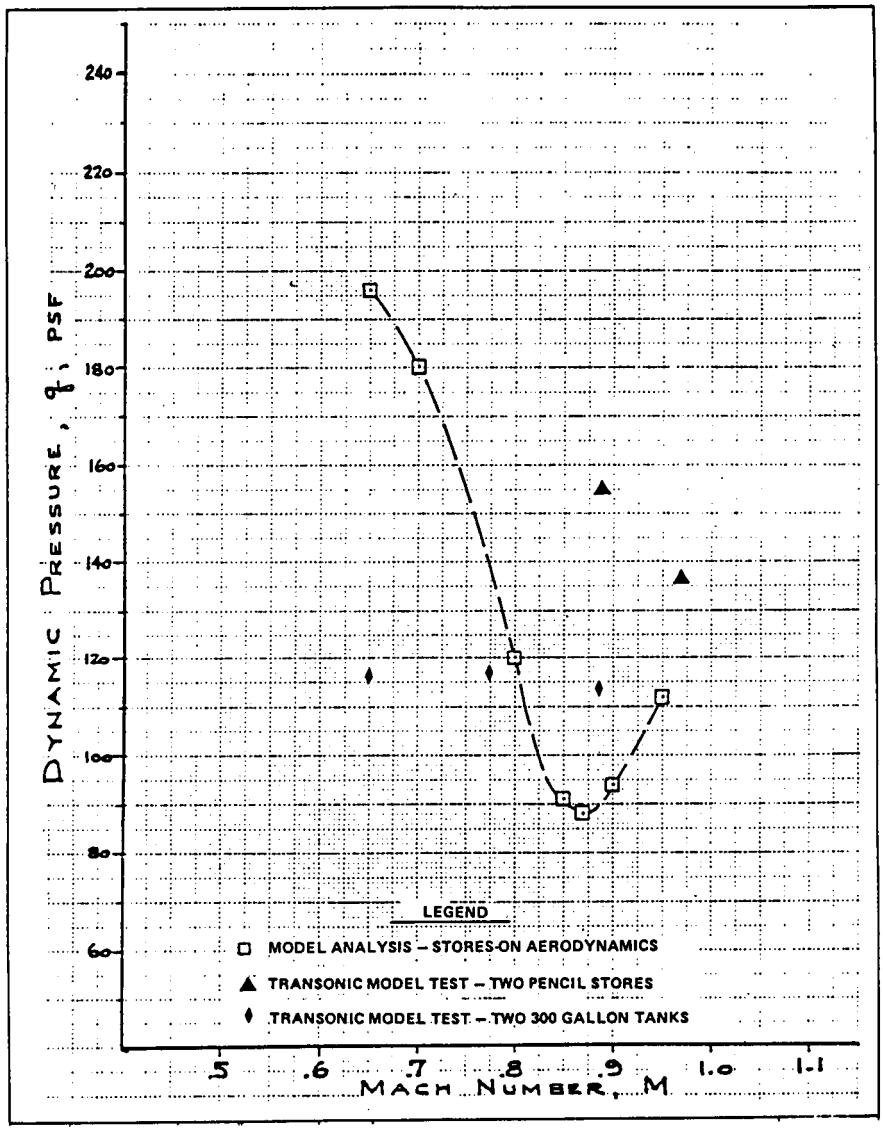

FLUTTER ANALYSIS,
TWO 300 GALLON TANKS ON PYLONS 4&5

INITIAL XTRAN3S STORE-PYLON SIMULATION

This figure shows a portion of the grid (Y-Z plane) used in the internal XTRAN3S simulation of the A-6 wing-pylon-store geometry. The pylons are located in planes midway between spanwise grid lines. The stores are simulated as a single line, with stores boundary conditions being satisfied at the four neighboring grid points. Shown in this figure are the maximum diameters of the 400 and 300 gallon tanks in relation to the wing and an approximate side of body location. The rigid model was tested with the store configuration shown plus a Sidewinder at the outboard station (which has not been modeled).

INITIAL XTRAN3S STORE-PYLON SIMULATION

(WING LOWER SURFACE)

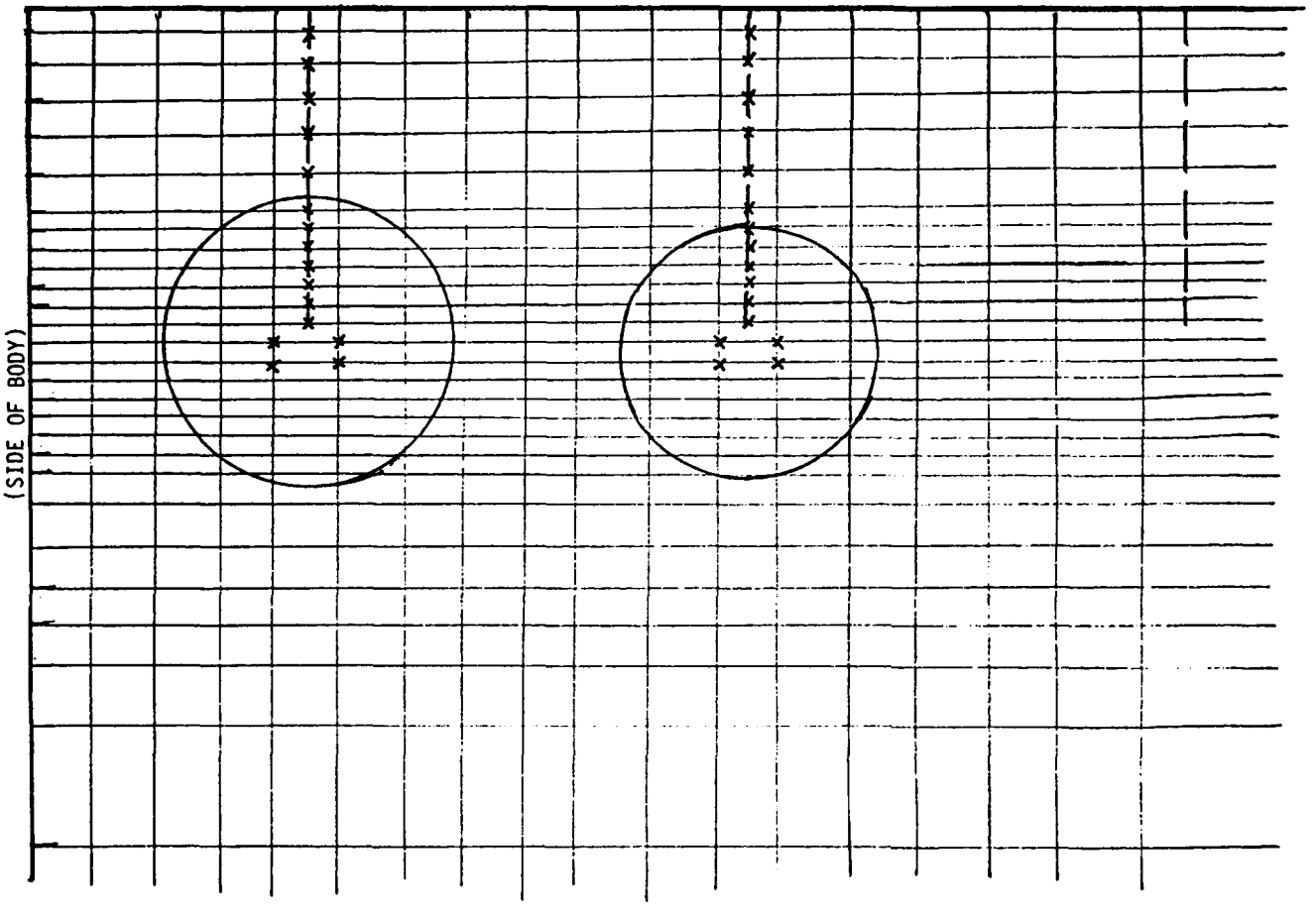

A-6 CLEAN WING

This figure and the next show the measured pressures on the wing upper and lower surface at a location just outboard of the inboard pylon station. Shown are the clean wing and pylons only cases. Also shown are the pressures predicted by XTRAN3S including surface boundary layers. Other than difference at the leading edge and slight pressure differences on the lower surface, the comparison is good.

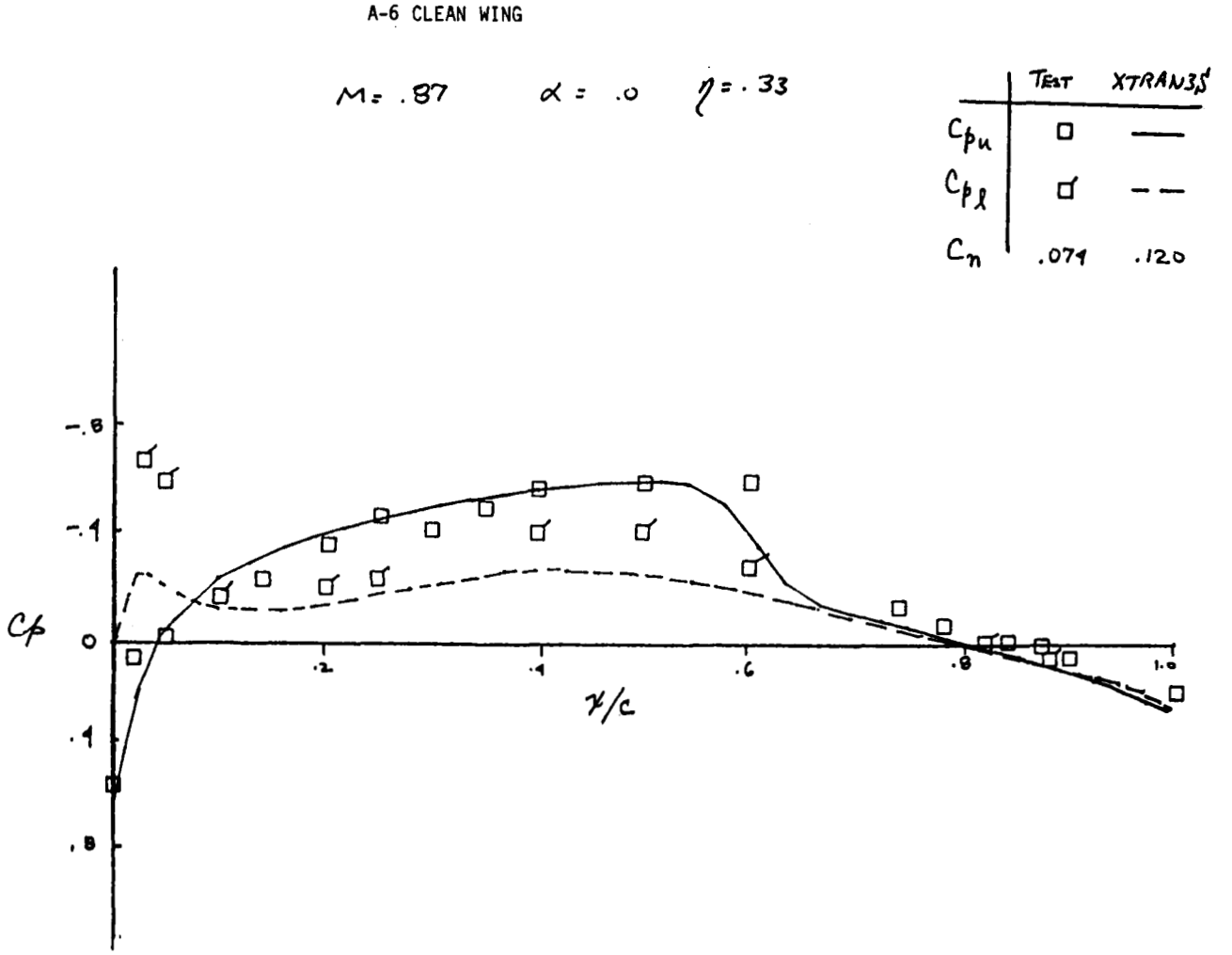

A-6 PYLONS ONLY

$M = .97 \quad \alpha = 0.0 \quad \eta = .33$

	TEST	XTRAN3S
C_{p_u}	□	——
C_{p_l}	□	— —
C_n	.103	.098

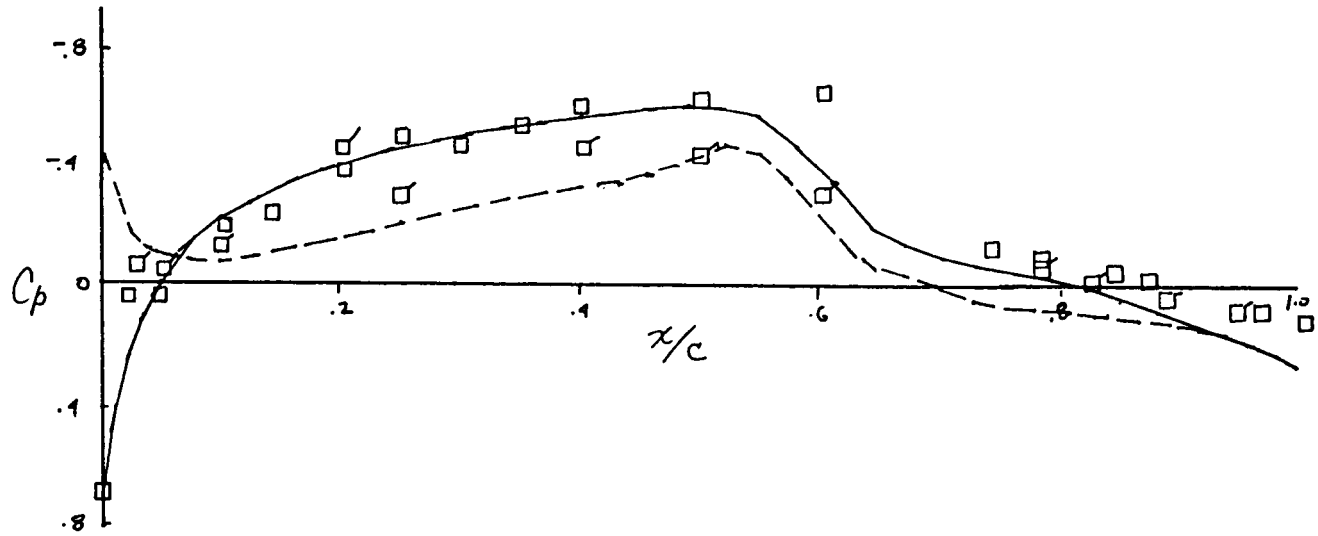

A-6 PYLON + STORES

This figure shows the comparison of measured and predicted pressures for the pylon-stores case. Although there is additional interference due to this "slender-body" modeling of the store, the comparison is neither qualitatively nor quantitatively good. Thus is was seen that a more complete modeling of the store is required.

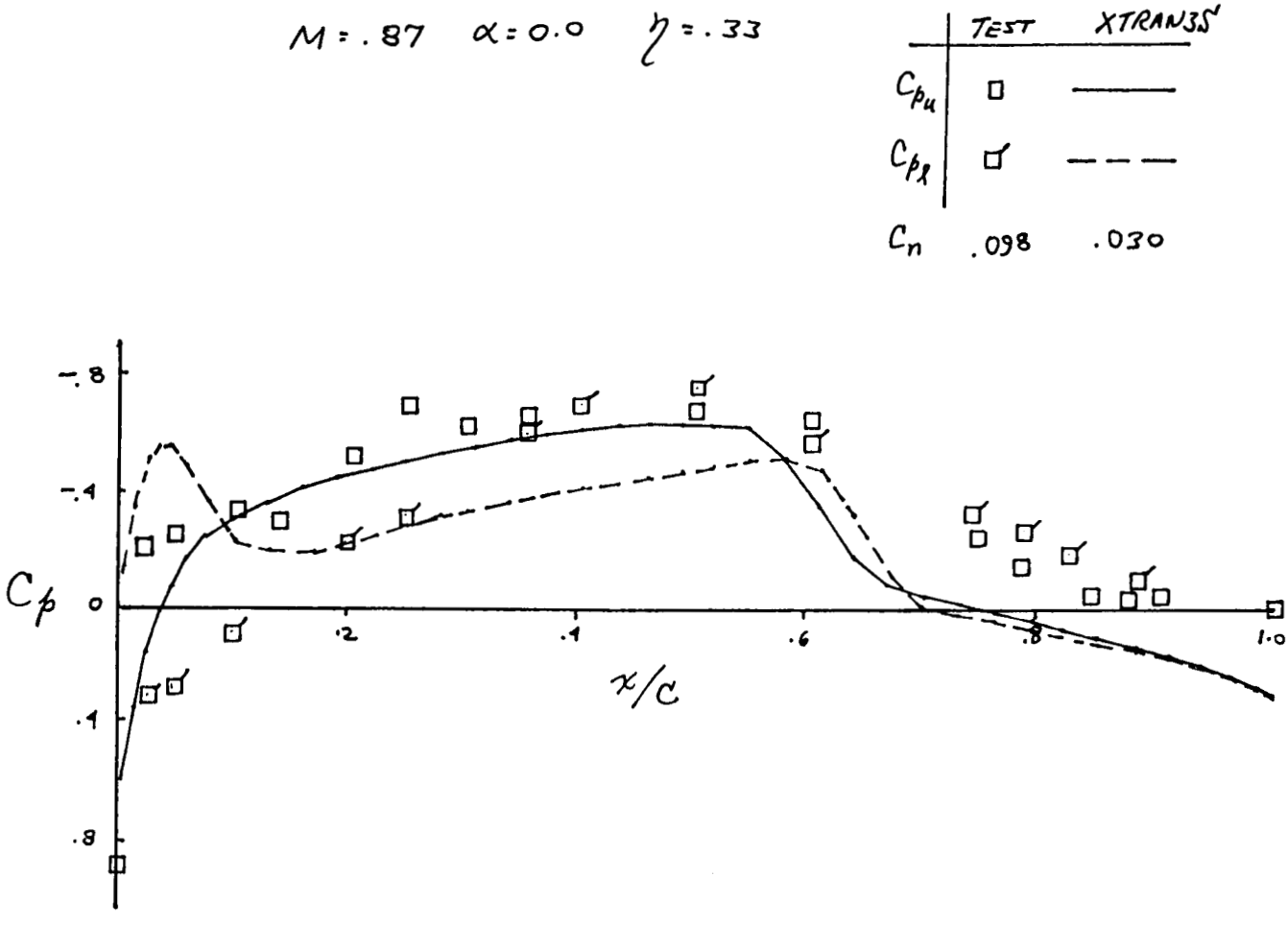

INTERFERENCE SHELL GEOMETRY

This figure shows the effective geometry of an "interference shell" or surface on which the boundary conditions are satisfied, surrounding the store. In the manner of Batina's Wing-Fuselage modification, slender-body corrections are used to modify the local surface boundary condition applied on the shell.

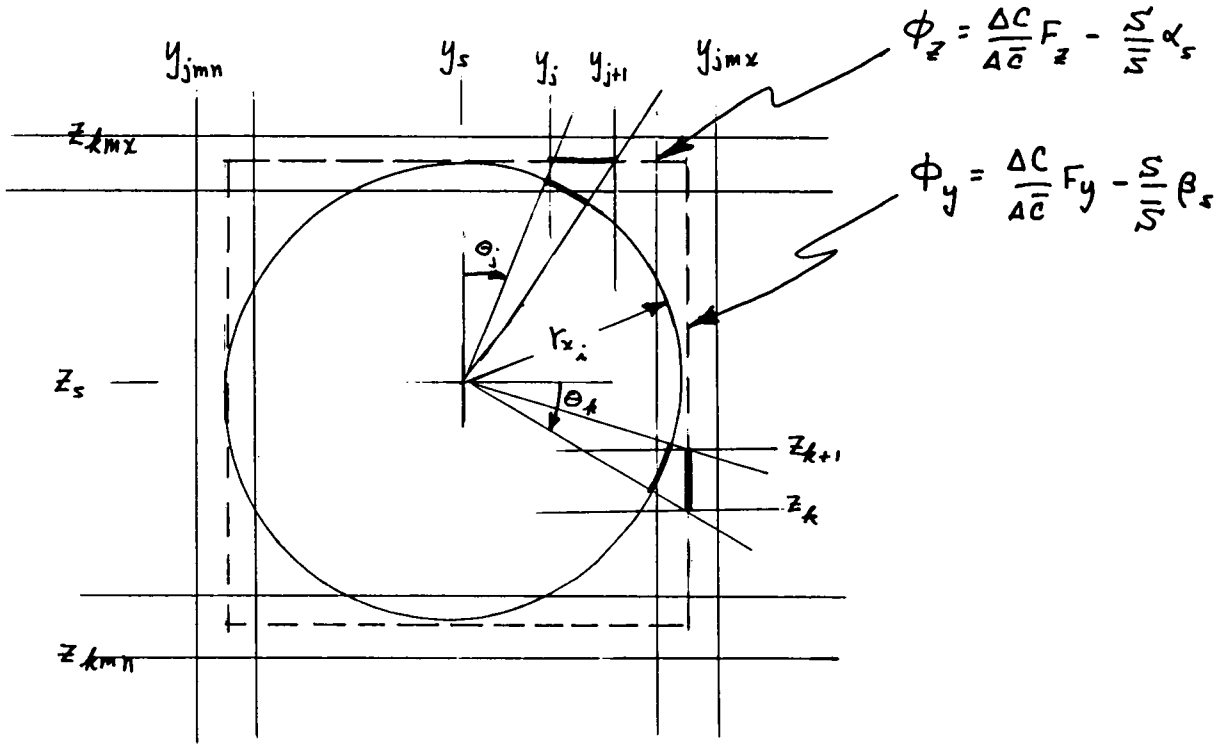

$$C_{ij} = r_{x_i} \left| \theta_{j+1} - \theta_j \right| \qquad S_i = \pi r_{x_i}^2$$

$$\bar{C}_i = y_{j+1} - y_j \qquad \bar{S}_i = (y_{jmx_i} - y \quad)(z_{kmx_k} - z_{kmn+1_k})$$

XTRAN3S STORE-PYLON SIMULATION

This figure shows the grid geometry for the store-pylon simulation with interference shells.

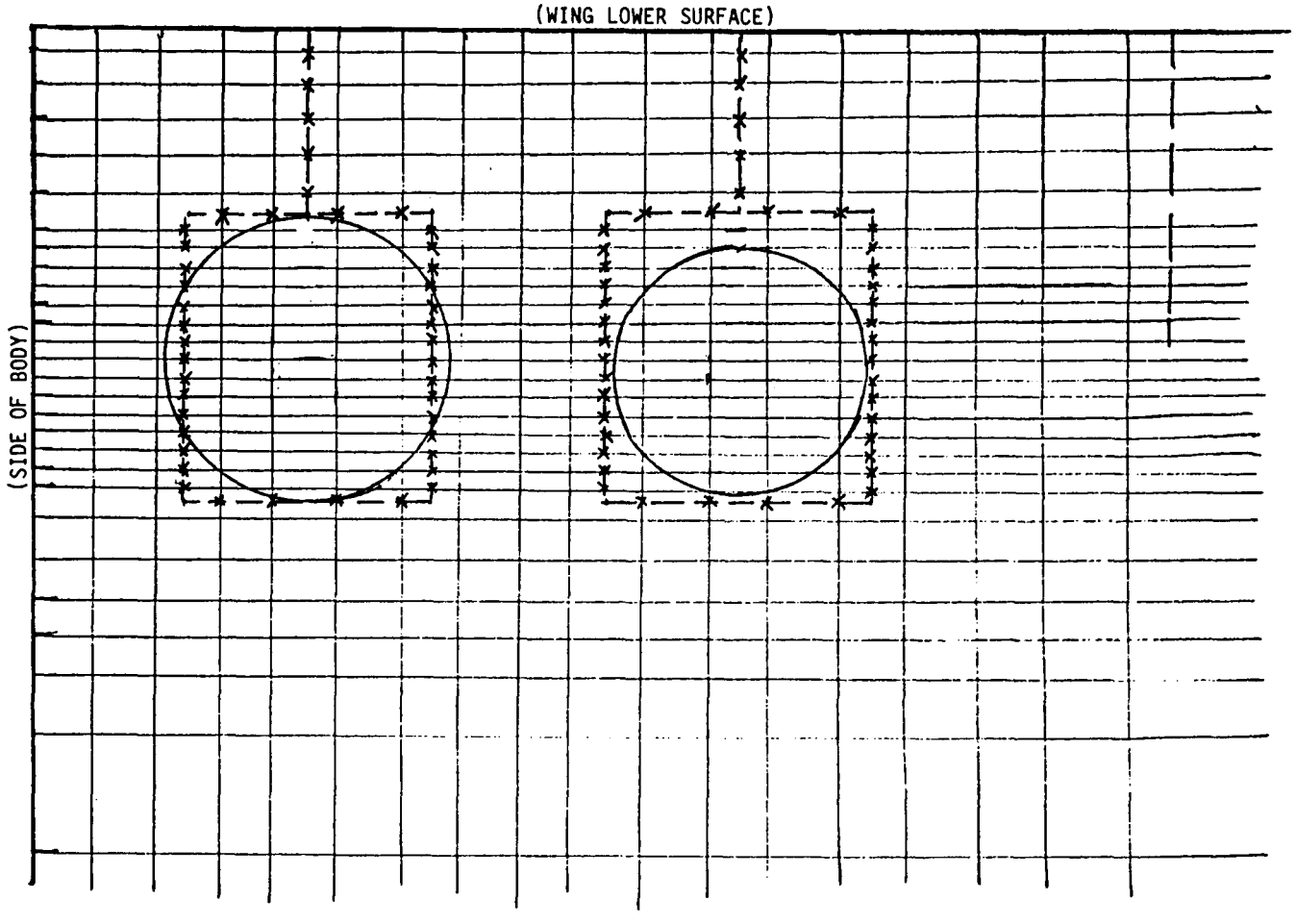

A-6 PYLONS + STORES (INTERFERENCE SHELL)

In this figure the XTRAN3S prediction with the interference shell is compared with measured data. The analysis predicts a much stronger shock, located closer to the trailing edge of the wing, than the data indicated. (The boundary layer calculation for this case was unstable; thus the result shown is an inviscid calculation.)

(At the symposium, the possibility of flow field separation causing the behavior shown was suggested by Joe Giesing of McDonnell-Douglas. This has been simulated and the results are shown in the next figure.)

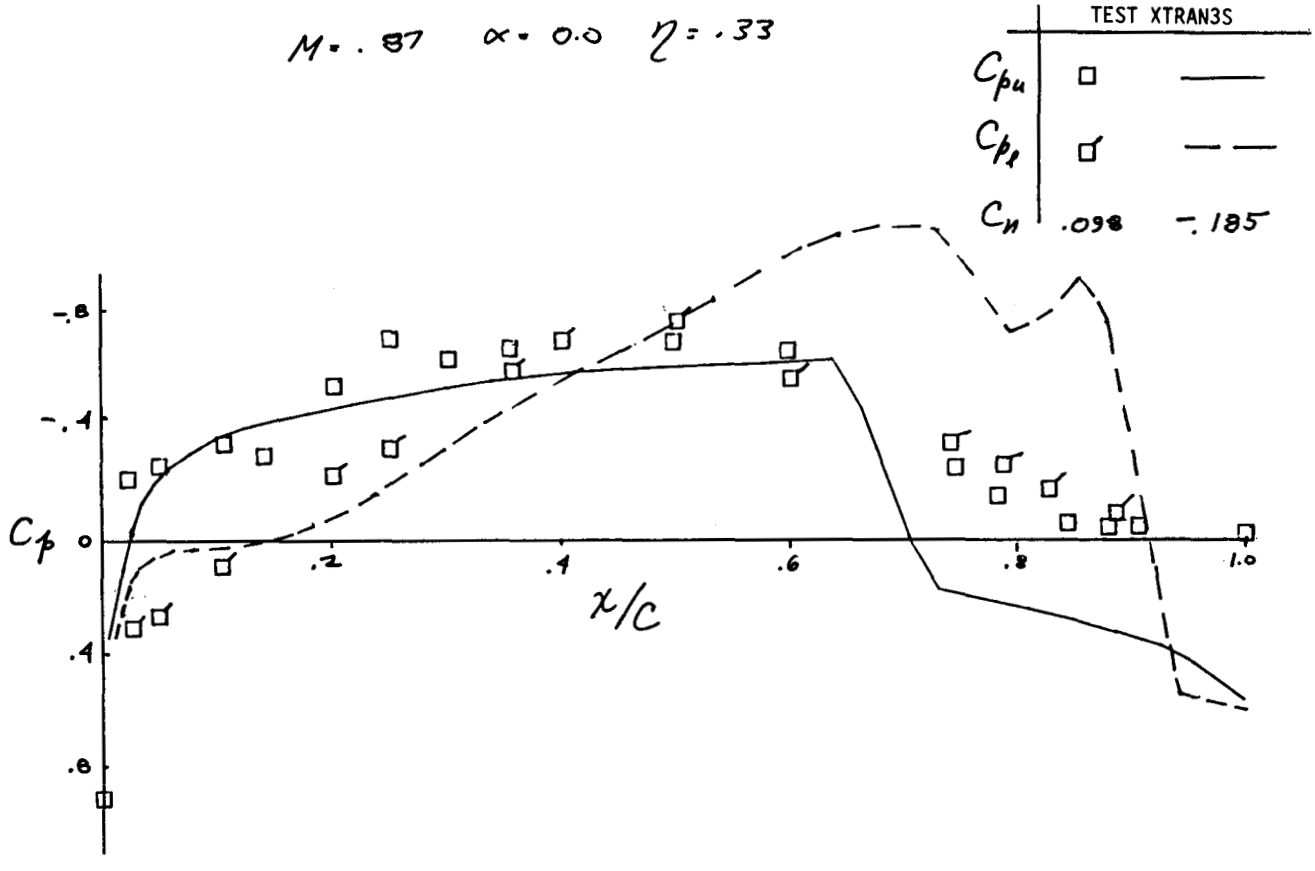

A-6 PYLON + STORES WITH AFT SEPARATION

Flow separation on the aft portion of the stores was simulated by use of a constant store radius and zero slope for the portion of the store aft of the maximum radius. This geometry modification has considerably improved the correlation with measured data, as shown in this figure. This calculation is shown with the boundary layer present. (This figure was not shown at the symposium.)

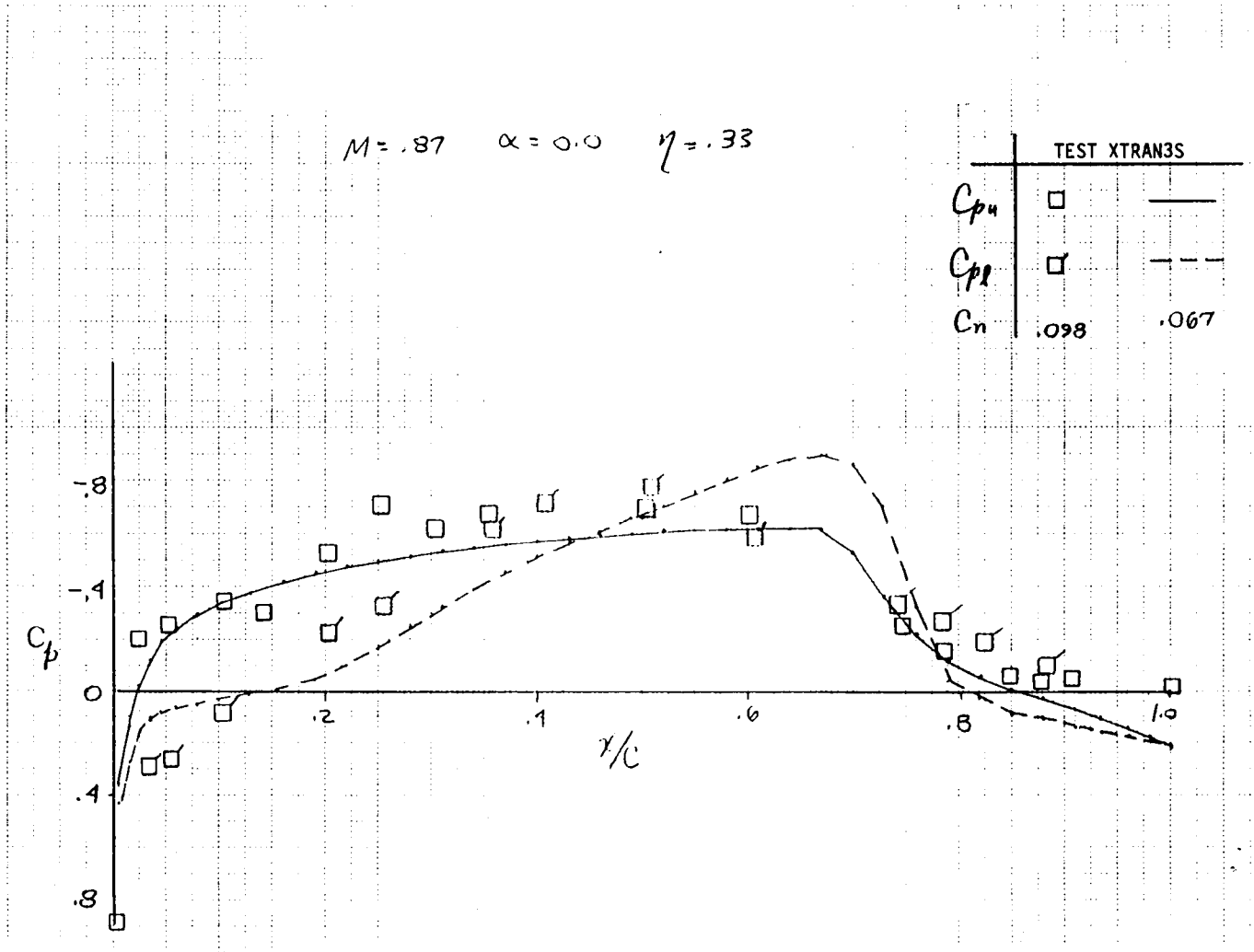

SUMMARY

In summary, modifications to the XTRAN3S code, implemented in Version 1.10, have provided a speed-up of twenty to thirty times over the previous released Version 1.5.

The pylon-store modification, under development, has shown that the presence of pylons and stores can be simulated although attention to geometric and flow field details is required.

- IMPROVED VECTORIZATION and ALGORITHM MODIFICATIONS PROVIDE 20-30X SPEED-UP IN XTRAN3S VERSION 1.10

- PYLON-STORE MODIFICATION DEVELOPED
  - SIMPLE SLENDER BODY INSUFFICIENT
  - INTERFERENCE SHELL OVERPREDICTS STORE INTERFERENCE ON WING

FUTURE EFFORTS

Future developments of the XTRAN3S code, to be initiated shortly under AFWAL sponsorship, are shown in this figure. Some comparisons with NASA-Langley's CAP-TSD code will be made at a later date.

- CONTINUE DEVELOPMENT ON PYLON-STORE MODIFICATION
- INCORPORATE WING-BODY AND PYLON-STORE MODIFICATIONS IN SINGLE VERSION
- ADD SUPERSONIC AND FOURIER ANALYSIS CAPABILITIES
- CONTINUE EVALUATIONS WITH TRANSPORT AND ATTACK AIRCRAFT AEROELASTIC MODELS